NJC

PAPER

View Article Online
View Journal



Cite this: DOI: 10.1039/c8nj02309c

# A protein-based mixed selector chiral monolithic stationary phase in capillary electrochromatography†

Shujuan Xu,[ab] Yuying Wang,[ab] Yixia Tang[ab] and Yibing Ji *[ab]

A new mixed selector chiral stationary phase (CSP) was prepared with co-immobilized human serum albumin and cellulase on a poly(glycidylmethacrylate-*co*-ethylene glycol dimethacrylate) (poly(GMA-*co*-EDMA)) monolith and the evaluation of its usefulness in chiral separation research was presented. For comparison, two single selector chiral stationary phases (CSPs) were also fabricated with the corresponding proteins. The enantioseparation ability of these CSPs was investigated by capillary electrochromatography (CEC) with various racemates. The mixed selector CSP exhibited a broader range of enantioselectivities than the single selectors and it could separate 10 chiral analytes while the two single selector CSPs resolved 3 and 8 respectively. Moreover, for (±)-warfarin, the enantioresolution was improved on the mixed selector CSP. Meanwhile, compared with the single selector CSPs, no additional preparation stage or reagent consumption was required in the simultaneous immobilization of different proteins, which is more favorable from economical and practical points of view. Consequently, by mixing HSA and cellulase together, the composite column combines the enantioselectivities of both individual proteins, thus expanding their application range practically.

Received 10th May 2018,
Accepted 9th July 2018

DOI: 10.1039/c8nj02309c

rsc.li/njc



## 1. Introduction

The enantioseparation of chiral drugs continues to be a hot topic in pharmaceutical analysis.[1,2] Among the various chromatographic separation techniques, capillary electrochromatography (CEC) has been widely utilized for chiral separation due to its important advantages over classical techniques, such as the minimization of solvent consumption, the reduced environmental impact, and the improved suitability for coupling with mass spectrometry detection.[3]

In CEC, one of the most significant topics of research in the field of chiral separation is the development of CSPs, along with high selectivity for a variety of compounds. Monoliths, bearing the advantages of easy preparation, low resistance to mass transfer and high permeability, have become ideal stationary phases for various separation formats. There are several chiral selectors that have been utilized in CEC with monoliths such as ligand exchangers,[4] Pirkle-type selectors,[5] cyclodextrin (CD) and its derivatives,[6] polysaccharide derivatives,[7] antibiotics,[8] chiral crown ethers[9] and proteins.[10] Among these, protein-based monoliths present high efficiency for enantiomeric separation due to multiple binding sites on the surface of the protein and multiple binding interactions between the protein and analyte. To date, various proteins, including bovine serum albumin (BSA),[11–14] human serum albumin (HSA),[15–18] penicillin G acylase,[19,20] $\alpha_1$-acid glycoprotein (AGP),[21] ovomucoid (OVM),[22] pepsin,[23–25] lipase[26] and avidin[27] have been successfully immobilized on monoliths as a chiral stationary phase in high-performance liquid chromatography (HPLC) or CEC. Though a wide range of racemic compounds have been resolved on these CSPs, the chiral recognition abilities of different proteins are markedly complementary. Therefore, the combination of two (or more) different proteins in one stationary phase may lead to a broader range of enantioselectivities than those provided by either of the single protein based stationary phases. However, a mixed chiral monolithic stationary phase containing different proteins as a selector has not been previously described.

HSA, a non-glycosylated protein, having an isoelectric point (pI) of 4.7 and a molecular mass of 66.5 kDa, is known to bind a variety of drugs and biological compounds.[28] When immobilized on a monolithic column, this can be used to study drug–protein interactions and separate some chiral solutes.[29] HSA-based monoliths, as obtained by anchoring the protein to a polymer or silica monolithic matrix, were first introduced by Hage and coworkers,[15] and these columns have been successfully applied to the enantiomeric separation of neutral and acidic drugs including tryptophan, phenylalanine, ibuprofen and warfarin by HPLC, while they exhibit much less efficiency for basic drugs.[15–17,30]

[a] Department of Analytical Chemistry, China Pharmaceutical University, Nanjing 210009, China. E-mail: jiyibing@msn.com
[b] Key Laboratory of Drug Quality Control and Pharmacovigilance, Ministry of Education, Nanjing 210009, China

† Electronic supplementary information (ESI) available. See DOI: 10.1039/c8nj02309c

Cellulase from *T. reesei* is a mixture of many hydrolytically active enzymes containing three main components: cellobiohydrolase I (CBH I), cellobiohydrolase II (CBH II) and endoglucanase II (EG II), whose molecular weights are 64 kDa, 53 kDa and 48 kDa, respectively and pIs are 3.9, 5.9 and 5.5, respectively.[31–33] Recently, Matsunaga *et al.* immobilized cellulase on aminopropyl-silica gels *via* its amino and carboxy groups respectively, by using *N*,*N*′-disuccinimidyl carbonate (DSC), and 1-ethyl-3-(3′-dimethylaminopropyl)carbodimide (EDC) and *N*-hydroxysulfosuccinimide (HSSI).[34] The new CSPs showed good selectivity and resolution in the enantioselective analysis of β-blockers, such as propranolol, alprenolol, oxprenolol and pindolol. In addition, the effect of silica particle diameters (5, 3 and 2.1 μm) on the chromatographic performance was also investigated and it was shown that the 2.1 μm aminopropyl-silica gels give the most efficient performance. Although smaller silica particles can improve the separation efficiency, the back-pressure increases rapidly with decreasing particle size. Compared with packed columns, monoliths, due to their porous properties, can avoid this effectively. Nevertheless, to the best of our knowledge, there has been little work reported on the use of monolithic columns for cellulase immobilization.

Considering the similar molecular mass and pI, as well as complementary enantioseparation scope of HSA and cellulase, in this work, we prepared a protein based mixed selector polymer monolithic CSP (HSA–cellulase@poly(GMA–EDMA) monolith) in order to extend the range of applications of single selector CSPs. GMA was used as a functional monomer that can be formed by the aminolysis of the epoxy groups and then activation with glutaraldehyde to anchor proteins. The enantioseparation ability of the newly prepared mixed selector CSP and corresponding single selector CSPs was evaluated by using different classes of racemic pharmaceuticals, namely, α- and β-blockers, serotonin-reuptake inhibitors, antihistamines, anticoagulants, and amino acids under the same separation conditions by CEC. Moreover, the factors that affect the separation efficiency including protein concentration, capillary inner diameter and CEC conditions were also investigated.

# 2. Experimental

## 2.1. Chemicals and materials

2,2′-Azobisisobutyronitrile (AIBN), *n*-propanol, 1,4-butanediol, sodium cyanoborohydride ($NaCNBH_3$), γ-methacryloxypropyltrimethoxylsilane (γ-MAPS), GMA, EDMA, glutaraldehyde, cellulase and tryptophan were purchased from Aladdin Chemistry (Shanghai, China). HPLC-grade methanol and acetonitrile (ACN) were from CINC High Purity Solvents (Shanghai) Co., Ltd (Shanghai, China) and Tedia Co. Inc. (OH, USA), respectively. Thiourea, ammonium hydroxide, phosphoric acid, hydrochloric acid and 2-propanol were commercially available from Nanjing Chemical Reagent Co., Ltd (Nanjing, China). Sodium hydroxide and disodium hydrogen phosphate dodecahydrate were from Xilong Chemical Co., Ltd (Shantou, China). HSA was from Sigma-Aldrich (Shanghai, China). Deionized water was used in all of the experiments, including synthetic reaction and mobile phase preparation. (±)-Azelastine was obtained from Jiangsu Hengrui Medicine Co., Ltd (Lianyungang, China). (±)-Warfarin was obtained from Nanjing Lide Biotechnology Co., Ltd (Nanjing, China). Other racemic drugs were from Dalian Meilun Biotec Co., Ltd (Dalian, China). Bare fused-silica capillaries (50, 75, 100 μm i.d. × 365 μm o.d.) were supplied by Yongnian Rui-feng Chromatographic Devices Co., Ltd (Handan, China).

## 2.2. Instruments

An Agilent 7100 CE system (Waldbronn, Germany) equipped with a diode-array UV detector, an auto-sampler, a ±30 kV power supply, a temperature controlled column compartment, an external nitrogen pressure, and a chromatographic workstation (Chemistry Station, USA) was used. SEM was carried out on a S-3400N II (Hitachi, Japan).

## 2.3. Preparation of the monolithic support

The scheme for preparation of the poly(GMA–EDMA) monolith is shown in Fig. 1A. The fused-silica capillary was washed with 1.0 mol $L^{-1}$ NaOH (1 h), 0.1 mol $L^{-1}$ HCl (30 min), and methanol (10 min) successively to activate the silanol groups on the capillary wall. The capillary was then dried by nitrogen gas for 2 h at 120 °C. In order to provide covalent attachment of the polymer, the pretreated capillary was then silanized by γ-MAPS (50%, v/v) in methanol and reacted at 50 °C overnight followed by a rinsing step with methanol and a drying step with nitrogen. To obtain a monolithic bed suitable for further experiments, a mixture of 21.96% (v/v) GMA, 7.47% (v/v) EDMA, 62.38% (v/v) *n*-propanol, 8.19% (v/v) 1,4-butanediol and 0.32% (m/v) AIBN was introduced into the preconditioned fused-silica capillary to the appropriate length by siphon action and reacted at 46 °C for 12 h. Finally, the resulting column was immensely flushed with methanol and water in order to remove the porogenic solvents and the unreacted monomers. To obtain sufficient quantities of the monolithic material for surface area determination and ninhydrin reaction, polymerization of the

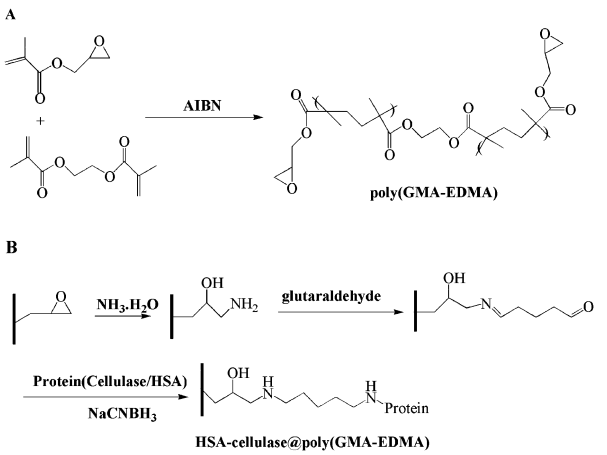


Fig. 1 General scheme for the preparation of the HSA–cellulase@poly(GMA–EDMA) monolith.

 

same reaction mixture was carried out in quartz tubes (180 mm × 3 mm i.d.) instead of a capillary tube under the same experimental conditions.

### 2.4. Immobilization of the proteins

The aminolysis of epoxy rings was carried out using 25% (m/v) ammonium hydroxide at 40 °C for 5 h. The activation with carbonyl groups was performed using a 50% glutaraldehyde solution (m/v) for 5 h at room temperature. Afterwards, the immobilization was carried out with a 4 mg $mL^{-1}$ protein mixture solution dissolved in 100 mmol $L^{-1}$ phosphate buffer (pH 7.0) containing 2 mg $mL^{-1}$ $NaCNBH_3$ for 12 h. The protein mixture consisted of HSA and cellulase at a concentration ratio of 1 : 1. Finally, the prepared monolithic column was washed with 100 mmol $L^{-1}$ phosphate buffer (pH 7.0) for 2 h to remove the nonspecifically absorbed proteins and then conditioned with running buffer for 1 h before installation to the CEC instrument. For comparison, the corresponding single selector chiral stationary phases (HSA@poly(GMA–EDMA) monolith and cellulase@poly(GMA–EDMA) monolith) were also fabricated with the two individual proteins at the concentration of 2 mg $mL^{-1}$ using the same procedure, respectively. The procedure of protein immobilization is shown in Fig. 1B.

### 2.5. Electrochromatography conditions

The mobile phase was 10 mmol $L^{-1}$ phosphate buffer solution with or without organic modifier. The phosphate buffer was freshly prepared by dissolving an exact amount of disodium hydrogen phosphate in deionized water and adjusted to a desired pH by phosphoric acid. The racemic drugs were dissolved in methanol or deionized water and diluted to an appropriate concentration. All above solutions were filtered through 0.22 μm nylon membrane filters and degassed before use. Unless stated otherwise, the monolithic columns (effective length 21 cm and total length 34 cm) were equilibrated prior to CEC runs with mobile phases until a stable current was observed. The column was thermostated at 20 °C and the applied voltage was in the range of 5–25 kV. Electrokinetic injections were adopted at 10 kV for 1 s or 2 s unless otherwise stated.

## 3. Results and discussion

### 3.1. Characterization of the prepared monolithic column

In CEC mode, the direction and magnitude of electroosmotic flow (EOF) reveal the property of the capillary columns. In order to confirm that the protein-based mixed selector chiral monolithic stationary phase has been successfully synthesized, thiourea was used as the EOF marker to measure the EOF after each step of the reaction. As seen in Fig. S1 (ESI†), in the pH range of 5.0–8.0, the EOF of the pristine poly(GMA–EDMA) monolith was too low to elute thiourea in 50 min due to the lack of groups that can generate EOF. After reaction with ammonium hydroxide, the $NH_2$@poly(GMA–EDMA) monolith generated a high reversed EOF from cathode to anode. The EOF decreased with the pH increasing from 5.0 to 8.0, because the protonated amino groups reduced. When the glutaraldehyde (GA) was reacted with amino to form imine, the EOF of the GA@poly(GMA–EDMA) monolith reduced. After HSA and cellulase were covalently immobilized to the GA@poly(GMA–EDMA) monolith, a positive EOF from the anode to the cathode was generated in the pH range of 6.0–8.0, which was attributed to the fact that HSA and cellulase were negatively charged. When the pH value was 5.0, the cellulase became positively charged and HSA had almost no charge, so the direction of EOF changed from cathode to anode. The above results should be interpreted as convincing proof of successful immobilization of HSA and cellulase onto the poly(GMA–EDMA) monolith.

Ninhydrin reaction was also carried out by treating the monolithic materials obtained from each step of the reaction with 0.2% ninhydrin (m/v) in ethanol. As seen in Fig. S2 (ESI†), the pristine poly(GMA–EDMA) monolith was still colorless when it was mixed with ninhydrin solution in a 100 °C water bath for a few minutes. For the $NH_2$@poly(GMA–EDMA) monolith, it was purple after being treated with ninhydrin, proving the successful modification with ammonium hydroxide. For the GA@poly(GMA–EDMA) monolith, the purple disappeared, suggesting the reaction between GA and amino-groups. For the HSA–cellulase@poly(GMA–EDMA) monolith, the purple appeared again, indicating that the protein has been modified on the monolith.

The morphology of the HSA–cellulase@poly(GMA–EDMA) monolith was investigated by SEM. As illustrated in Fig. 2, the prepared monolith was homogeneous and tightly anchored to the capillary wall without any disconnection. The large through pores presented in this stationary phase could reduce the flow resistance. This would guarantee effective mass transfer and high stability of the fabricated column. The porous properties of the prepared monoliths were also investigated. The specific surface area was measured by nitrogen adsorption on a Micromeritics ASAP 2020 V4.00 (Micromeritics, USA). As described in the previous studies,[35,36] total porosity was estimated by using the gravimetric method and the permeability was determined based on Darcy's Law with water as the

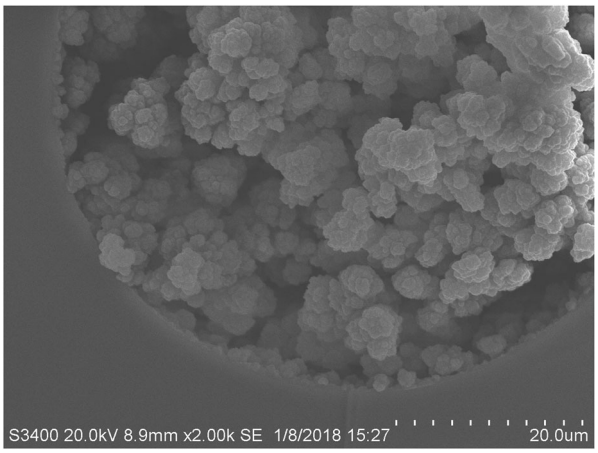


Fig. 2 Scanning electron micrograph for the HSA–cellulase@poly(GMA–EDMA) monolith.

eluent at room temperature. The effective radius of the equivalent pores was calculated using the Kozeny–Carman equation. The numerical values for the specific surface area, porosity, pore diameter and permeability were 3.33 $m^2$ $g^{-1}$, 0.57, 3.6 μm and 3.7 × $10^{-13}$ $m^2$, respectively.

### 3.2. Enantioseparation on the HSA–cellulase@poly(GMA–EDMA) monolith

**3.2.1. Effect of protein concentration on enantioseparation.** The concentration of protein could affect the amounts of protein immobilized on the monolith. As a result, the separation performance of the HSA–cellulase@poly(GMA–EDMA) monolith may also be affected by the protein concentration. Thus, the effect of protein concentration on the enantioseparation effectiveness was investigated. As seen in Fig. 3, the resolution ($R_s$) and selectivity factor (α) of (±)-metoprolol, the model analyte, increased firstly and then decreased with the increase in the concentration of protein from 2 to 8 mg $mL^{-1}$. When the protein concentration was 4 mg $mL^{-1}$, the $R_s$ and α reached the maximum. However, for (±)-tryptophan the $R_s$ and α were increased by increasing the content of protein. The $R_s$ (1.43, 2.12, 2.28) and α (1.06, 1.12, 1.15) were observed for 2, 4, and 8 mg $mL^{-1}$ protein respectively. From section 3.4, we know the enantiorecognition of (±)-metoprolol comes from cellulase and only the HSA can resolve (±)-tryptophan, so the above phenomenon may be due to the fact that HSA could occupy more aldehyde binding sites at higher protein concentration thus leading to the reduction of immobilized cellulase. Meanwhile, a further increase of protein concentration resulted in lower column efficiency. From the viewpoints of higher resolution and column efficiency, the protein concentration of 4 mg $mL^{-1}$ was chosen in this study. In addition, the concentration ratios of HSA to cellulase at 1 : 2, 1 : 1 and 2 : 1 were also investigated. As seen in Fig. S3 (ESI†), the resolution of (±)-tryptophan increased with the HSA ratio increasing while the resolution of (±)-metoprolol increased with the increase in cellulase ratio. Taking into account both, the optimum concentration ratio of HSA to cellulase was determined to be 1 : 1.

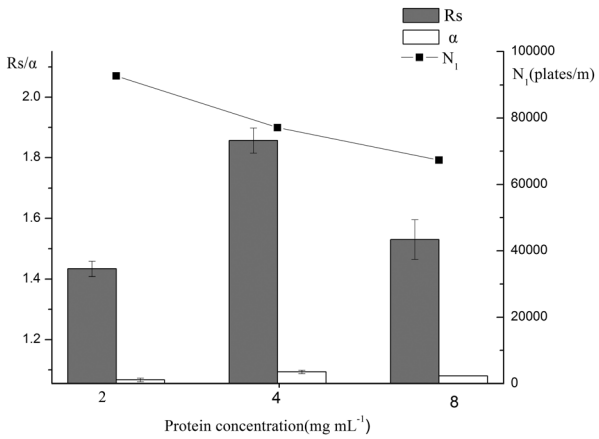


Fig. 3 Effect of protein concentration on enantioseparation of (±)-metoprolol on the HSA–cellulase@poly(GMA–EDMA) monolith. Experimental conditions: $R_s$, resolution; α, selectivity factor; $N_1$, plate count for the first-eluting enantiomer; samples, 50 μg $mL^{-1}$ (±)-metoprolol; running buffer, 10 mmol $L^{-1}$ phosphate buffer (pH 7.0, containing 10% 2-propanol); applied voltage, 10 kV; injection, 10 kV × 2 s; detection wavelength, 225 nm; temperature, 20 °C.

**3.2.2. Effect of capillary inner diameter on enantioseparation.** The influence of the capillary inner diameter (50, 75 and 100 μm) on column performance was investigated in detail. As shown in Fig. 4, the current and electroosmotic flow (EOF) of the HSA–cellulase@poly(GMA–EDMA) monolith increased with the capillary inner diameter increasing while the column back pressure decreased (the column back pressure was observed when the flow rate was 3 μL $min^{-1}$ using water as the mobile phase). In comparison with the 50 μm i.d. column, the 75 μm i.d. column could provide more immobilization sites to load proteins (3.35, 5.55 and 6.81 μg of proteins were immobilized on 1 cm length HSA–cellulase@poly(GMA–EDMA) monoliths prepared with 50 μm, 75 μm and 100 μm inner diameter capillaries, respectively, see Fig. S4, ESI†), which strengthened the interaction between the proteins and (±)-metoprolol, consequently leading to higher resolution. Whereas, when the inner diameter was increased to 100 μm, baseline separation of (±)-metoprolol could not be

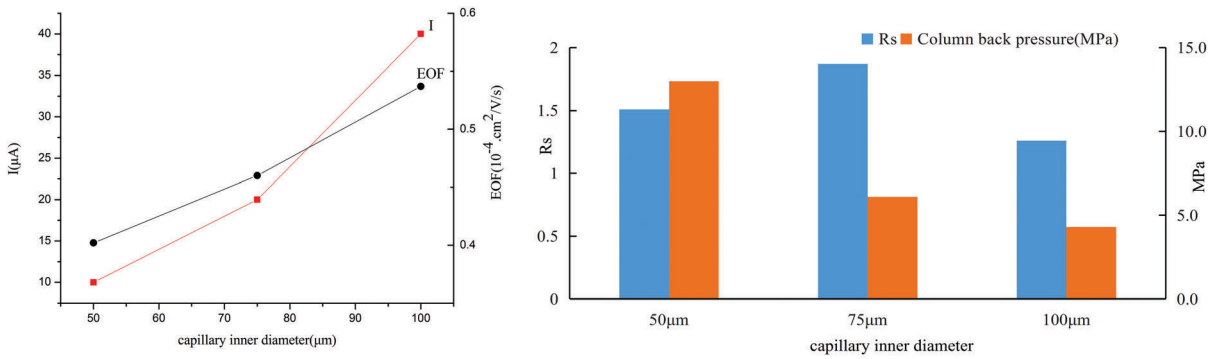


Fig. 4 Effect of capillary inner diameter on column performance of the HSA–cellulase@poly(GMA–EDMA) monolith. Thiourea was used as the EOF marker. Experimental conditions: samples, 50 μg $mL^{-1}$ (±)-metoprolol; running buffer, 10 mmol $L^{-1}$ phosphate buffer (pH 7.0, containing 10% 2-propanol); applied voltage, 10 kV for (±)-metoprolol and 20 kV for thiourea; injection, 10 kV × 2 s for (±)-metoprolol and 10 kV × 1 s for thiourea; detection wavelength, 225 nm for (±)-metoprolol and 210 nm for thiourea; temperature, 20 °C. The back pressures were observed when the flow rate was 3 μL $min^{-1}$ using water as the mobile phase.

 

obtained and the peaks obviously broadened, which was attributed to the large temperature gradients that existed in wider capillaries.[37,38] Hence, the 75 μm inner diameter HSA–cellulase@poly(GMA–EDMA) capillary monolithic column was chosen.

**3.2.3. Effect of organic modifiers on enantioseparation.** Since organic modifiers can alter the enantioseparation by influencing interactions involved in the chiral recognition mechanism and EOF,[8] an organic modifier was considered to be added into the buffer in order to achieve baseline separation. The chiral separation of (±)-metoprolol was achieved in 10 mmol $L^{-1}$ phosphate buffer with 0 to 14% 2-propanol and the effect of 2-propanol on EOF, retention time ($t_R$), $R_s$ and α is illustrated in Table S1 (ESI†). With the increase of 2-propanol percentage, EOF exhibited a decreasing tendency, which can be explained by the change of dielectric constant/viscosity ratio and the influence of mobile phase polarity on the zeta potential.[39] For (±)-metoprolol, an increase in the retention time and resolution was observed when 2-propanol increased from 0% to 10%. It is obvious to note that the longer retention time was ascribed to the decrease in EOF. The addition of 2-propanol increased the affinity of the enantiomers for the chiral selector, hence strengthening the interaction between the enantiomers and the chiral stationary phase. However, by further increasing the 2-propanol concentration to 14%, the $R_s$ lowered due to the second peak broadening. Therefore, 10% 2-propanol was chosen for further investigation.

**3.2.4. Effect of pH on enantioseparation.** The pH of the running buffer could directly influence the ionization state of the analyte and the EOF within the column; therefore, a change in pH could have a great influence on chiral separation by CEC. The effect of pH from 6.5 to 8.5 on the enantioseparation of (±)-metoprolol was evaluated. As shown in Fig. 5, when the buffer pH increased, the retention time of metoprolol was gradually shortened, owing to the increasing EOF. On the other hand, the enantioselectivity increased when the buffer pH changed from 6.5 to 8.0, indicating that the interacting differences of two metoprolol enantiomers with the protein would be enhanced as the ionization degree of the protein increased. Conversely, the column efficiency decreased with increasing pH. This is probably because the enhanced interaction intensifies the tailing of the peaks. Under the double influence of α and column efficiency, the $R_s$ reached the maximum at pH 7.0. Further increasing the pH to 8.5, obviously poor enantioselectivity occurred, which may be due to the fact that the stability of the protein would be adversely affected at pH 8.5. Therefore, the optimum pH of the running buffer was determined to be 7.0.

**3.2.5. Effect of buffer concentration on enantioseparation.** Since the concentration of buffer solution can affect the buffering capacity, the resolution and column efficiency, the effect of the phosphate buffer concentration (from 5 to 20 mmol $L^{-1}$) on enantioseparation of metoprolol enantiomers was evaluated. As illustrated in Fig. S5 (ESI†), the retention time of (±)-metoprolol was gradually prolonged with increasing buffer concentration, due to the reduced zeta potential as usually observed in CEC. Resolution was increased with increasing buffer concentration up to 10 mmol $L^{-1}$. A further increase in buffer concentration gave declined resolution, which is likely due to the weakened electrostatic interaction between protein and (±)-metoprolol. Hence, a buffer concentration of 10 mmol $L^{-1}$ was chosen for further analysis.

**3.2.6. Effect of applied voltage on enantioseparation.** The effect of applied voltage in the range of 5–25 kV on the enantioseparation of (±)-metoprolol was evaluated and the results are presented in Fig. S6 (ESI†). As expected, when the applied voltage increased, the EOF was increased so that the retention time of (±)-metoprolol reduced. The resolution values were decreased upon the increase of voltage probably because of extra Joule heating and peak broadening. In addition, as the voltage increased, especially when the voltage exceeded 20 kV, the voltage and current deviated linearly, indicating an increase in Joule heat. To reduce the effect of Joule heating, a lower voltage should be used. In consideration of good resolution, shorter retention time and higher column efficiency, 10 kV was selected as the appropriate voltage for the separation of metoprolol enantiomers.

### 3.3. Stability and repeatability

Based on the relative standard deviations (RSD) of retention time and resolution of metoprolol enantiomers, the repeatability of the HSA–cellulase@poly(GMA–EDMA) monolith was evaluated. For the intra-day repeatability test, the racemic metoprolol

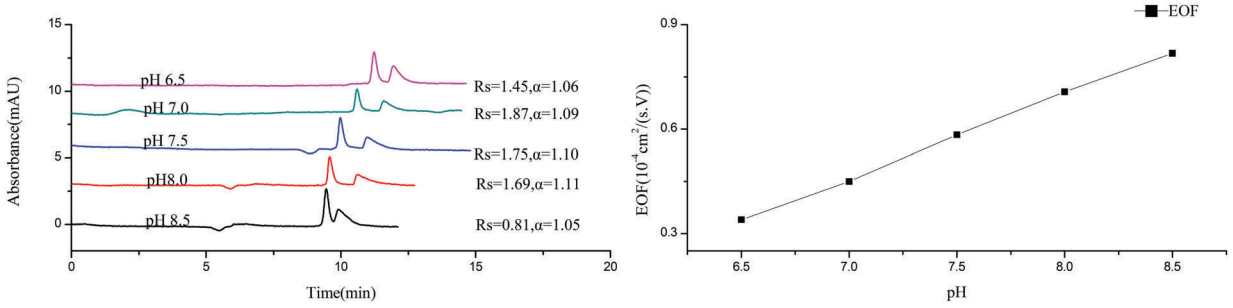


Fig. 5 Effect of pH on the chiral separation of (±)-metoprolol on the HSA–cellulase@poly(GMA–EDMA) monolith. Experimental conditions: samples, 50 μg $mL^{-1}$ (±)-metoprolol; running buffer, 10 mmol $L^{-1}$ phosphate buffer (pH 6.5–8.5, containing 10% 2-propanol), other conditions are the same as in Fig. 4.

standard solution was analyzed using five replicates within one day. The assessment of inter-day repeatability was carried out with a single capillary and it was performed by conducting three runs for three consecutive days. As for the column-to-column repeatability, the same test analyte was analyzed on three columns made from one polymerization mixture. Batch-to-batch repeatability was evaluated by another three columns that were fabricated from three polymerization mixtures prepared using the same method. The intra-day, inter-day, column-to-column and batch-to-batch RSD of the analyte's retention time and resolution shown in Table 1 were all less than 2.1% and 5.4%, which confirmed the good repeatability of the HSA–cellulase@poly(GMA–EDMA) monolith. Moreover, after 60 runs over 30 days on the column, little changes in resolution (only from 1.89 to 1.73) were observed and the intra-day repeatability was still good (the RSD values of retention time and resolution were 1.4% and 3.9%), suggesting good stability of the prepared polymer monolith.

Table 1 Repeatability data for the HSA–cellulase@poly(GMA–EDMA) monolith

| | $R_s$(avg), (% RSD) | $t_1$(avg), min (% RSD) | $t_2$(avg), min (% RSD) |
|---|---|---|---|
| Intraday ($n$ = 5) | 3.7 | 1.1 | 0.82 |
| Interday ($n$ = 9) | 4.4 | 1.5 | 1.6 |
| Column-to-column ($n$ = 9) | 4.2 | 1.9 | 2.1 |
| Batch-to-batch ($n$ = 9) | 5.4 | 1.1 | 1.9 |

Experimental conditions are the same as in Fig. 3.

### 3.4. Comparison with the corresponding single selector chiral stationary phases

The chiral recognition ability of the HSA–cellulase@poly(GMA–EDMA) monolith was evaluated by different classes of enantiomers including amino acid, basic and acid chiral drugs. In the experiment, there were ten enantiomers that could be enantioseparated on the HSA–cellulase@poly(GMA–EDMA) monolith and six of them could be completely resolved. For comparison, the corresponding single selector CSPs were also fabricated with the individual HSA and cellulase, respectively. As illustrated in Fig. 6, the mixed selector CSP could separate 10 chiral analytes, while the two single selector CSPs resolved 3 and 8 respectively. It is demonstrated that the mixed selector CSP exhibited a broader range of enantioselectivities than the single selectors.

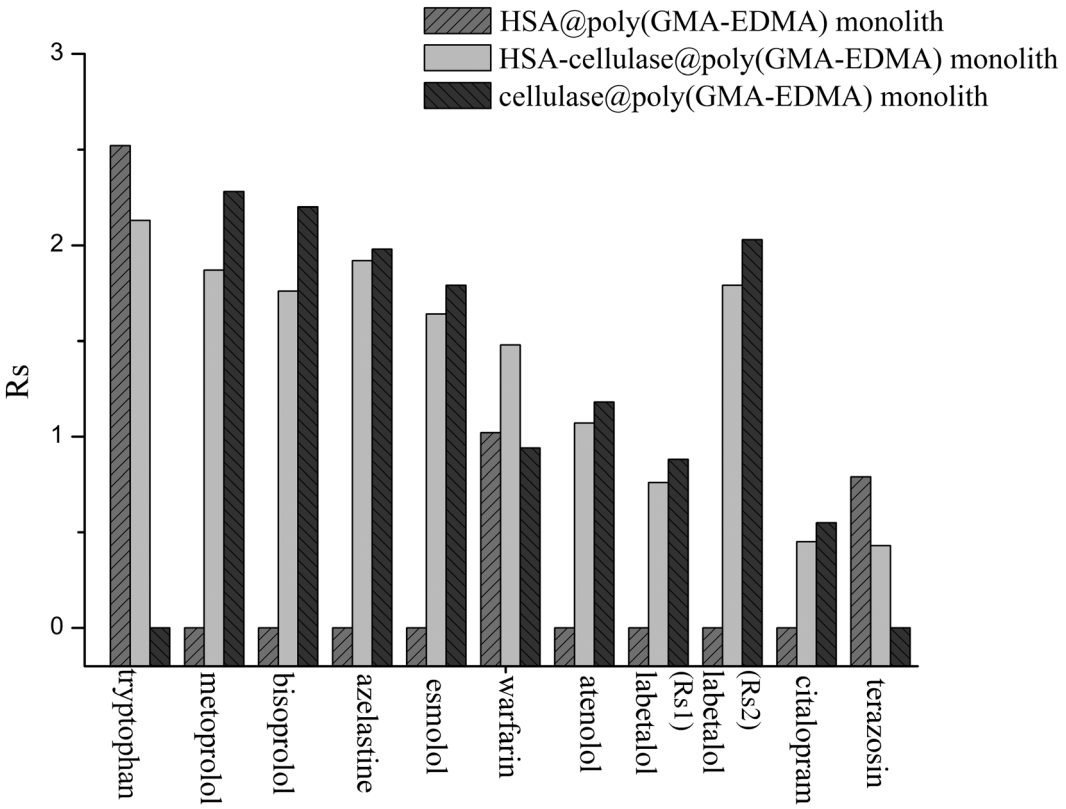


Fig. 6 Resolution of ten pairs of enantiomers on the HSA–cellulase@poly(GMA–EDMA) monolith, HSA@poly(GMA–EDMA) monolith and cellulase@poly(GMA–EDMA) monolith. Experimental conditions: samples, 0.7 mg $mL^{-1}$ (±)-tryptophan, 50 μg $mL^{-1}$ (±)-metoprolol, 0.1 mg $mL^{-1}$ (±)-bisoprolol, 0.2 mg $mL^{-1}$ (±)-azelastine, 0.1 mg $mL^{-1}$ (±)-esmolol, 1 mg $mL^{-1}$ (±)-warfarin, 0.1 mg $mL^{-1}$ (±)-atenolol, 0.1 mg $mL^{-1}$ (±)-labetalol, 30 μg $mL^{-1}$ (±)-citalopram and 50 μg $mL^{-1}$ (±)-terazosin; running buffer, 10 mmol $L^{-1}$ phosphate buffer (pH 7.0, without organic modifier for tryptophan, with 20% ACN for warfarin and with 10% 2-propanol for others); applied voltage, 20 kV for azelastine, terazosin, 15 kV for tryptophan, labetalol, warfarin and 10 kV for others; injection, 10 kV × 2 s for metoprolol, bisoprolol, labetalol, esmolol, warfarin, 1 kV × 2 s for atenolol, and 10 kV × 1 s for others; detection wavelength, 215 nm for azelastine, tryptophan, labetalol, warfarin, 254 nm for terazosin, 240 nm for citalopram and 225 nm for others; temperature, 20 °C.

 

Except for (±)-warfarin, the resolution for racemates that could be enantiomerically separated by just one of the two selectors, was slightly lower on such mixed CSP, because the content of this selector in the mixed CSP is actually lower than the phase containing such a selector only. For (±)-tryptophan, (±)-metoprolol, (±)-bisoprolol, (±)-esmolol and (±)-azelastine, the resolution values on the mixed selector CSP were all greater than 1.5, completely meeting the general separation requirements. Moreover, for (±)-warfarin, the chiral recognition capacity was improved on the mixed selector CSP, which might be brought about from the same elution order of enantiomers resolved by the two individual selectors. In such a case, the two selectors on a mixed CSP worked in a coordinative way that promoted the resolution. In general, by mixing HSA and cellulase together, the composite column combines the enantioselectivities of both individual proteins, thus expanding their application

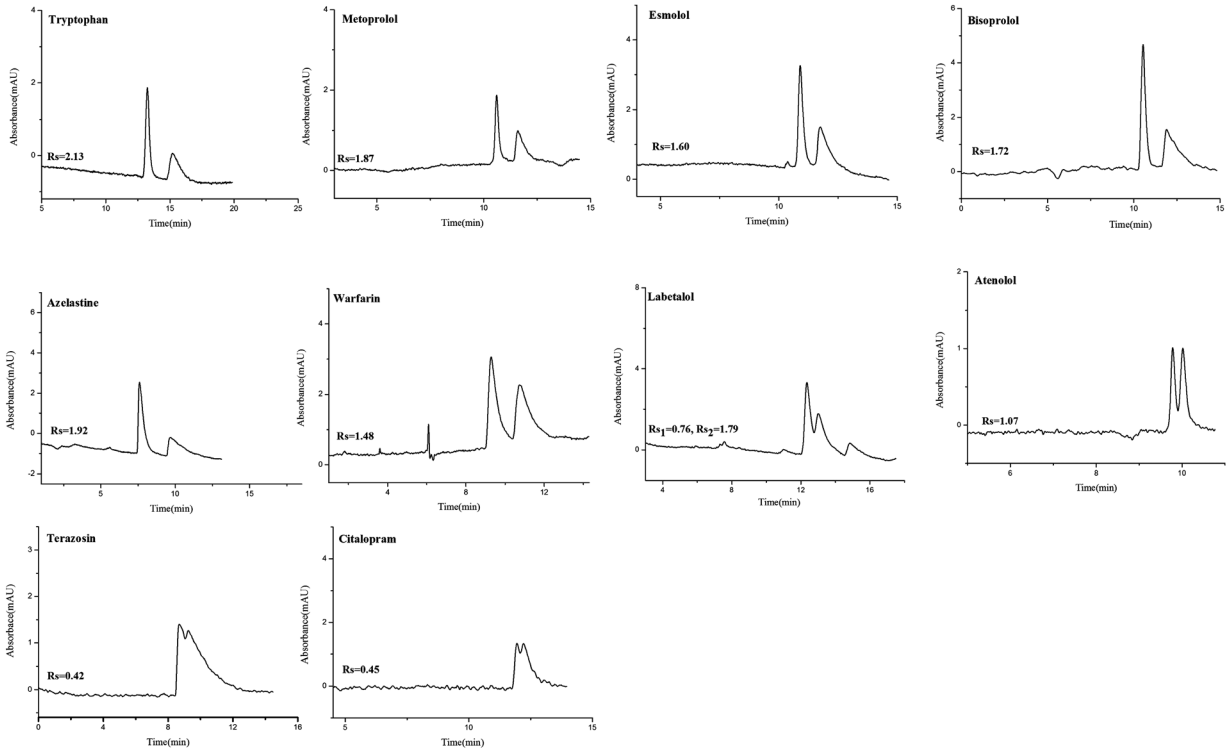


Fig. 7 Electrochromatograms for enantioseparation of ten chiral analytes on the HSA–cellulase@poly(GMA–EDMA) monolith. The conditions are the same as in Fig. 6.

Table 2 Comparison of serum albumin or cellulase based CSPs

| Backbone/methods | Types of protein | Analyte | Ref. |
|---|---|---|---|
| Poly(GMA–EDMA) monolith; HPLC | HSA | Warfarin, tryptophan | 15 |
| Poly(GMA–EDMA) monolith; HPLC | HSA | Tryptophan, phenylalanine | 16 |
| Poly(GMA–EDMA) monolith/ poly(GMA-TRIM) monolith; HPLC | HSA | Warfarin, tryptophan | 17 |
| GO modified silica monolith; CEC | HSA | Warfarin, tryptophan, salbutamol, chlortrimeton, propranolol, nefopam, phenylalanine, azelastine, ibuprofen (with GO); tryptophan, nefopam, azelastine (without GO) | 18 |
| Silica monolith; HPLC | HSA | Warfarin, tryptophan, ibuprofen | 30 |
| Silica monolith; CEC | BSA | Tryptophan, benzoin | 40 |
| Silica monolith; CEC | BSA | Tryptophan | 11 |
| Hybrid monolith; CEC | BSA | Tryptophan | 12 |
| Gold nanoparticle (GNPs) modified silica monolith; CEC | BSA | Phenylthiocarbamyl amino acids | 13 |
| Silica monolith; CEC | BSA | Tryptophan, pantoprazole, atenolol | 14 |
| Polystyrene nanoparticles; open-tubular CEC (OT-CEC) | BSA | Tyrosine, tryptophan, warfarin | 41 |
| GNPs; OT-CEC | BSA | FITC-labeled ephedrine and norephedrine | 42 |
| Silica gels; HPLC | Cellulase | Propranolol, alprenolol, oxprenolol, pindolol | 34 |
| Poly(GMA–EDMA) monolith; CEC | HSA and cellulase | Warfarin, tryptophan, terazosin, azelastine, atenolol, metoprolol, bisoprolol, esmolol, citalopram, labetalol | This work |

range practically. Fig. 7 shows the resultant enantioseparation electrochromatograms of ten chiral analytes on the HSA–cellulase@poly(GMA–EDMA) monolith.

### 3.5. Comparison of the work with previous reports

In previous reports, various serum albumin (HSA and BSA) or cellulase based CSPs have been successfully applied for enantioseparation research. It would be meaningful to compare the analytical feature of the present method with other previous reports. As shown in Table 2, an obvious wider range of chiral recognition ability was obtained on the HSA–cellulase@poly(GMA–EDMA) monolith with high column efficiency and low reagent consumption except for research.[18] In research,[18] the introduction of graphene oxide (GO) improved the chiral selectivity and the scope of the chiral drugs that could be separated by HSA was extended. However, without GO, there were only three enantiomers that could be resolved on the HSA based silica monolith, much less than on the HSA–cellulase@poly(GMA–EDMA) monolith. Furthermore, it is worth mentioning that the results acquired from the enantiomeric separation of tryptophan and warfarin in this work were better than the related research[18] considering the resolution and separation efficiency. This implied that the HSA–cellulase@poly(GMA–EDMA) monolith could be expected to be a promising microscale enantioseparation device.

## 4. Conclusions

In this work, a novel HSA–cellulase@poly(GMA–EDMA) monolith was successfully prepared and used as a stationary phase for enantioseparation by CEC. The prepared column exhibited powerful enantioseparation capability towards different chemical classes and there were ten chiral compounds that could be separated on this column. Compared with the individual HSA or cellulase based CSPs, the HSA–cellulase@poly(GMA–EDMA) monolith has an even wider range of applications. These results indicated that mixed selector CSPs combining the enantioselectivities of individual CSPs could be a useful tool for chiral separation, particularly in the simultaneous analysis of racemic mixtures that can only be resolved on different stationary phases. Further study will include covalently bonding other proteins onto the monolith to create other CSPs for the separation of different kinds of chiral compounds in the same capillary. Additionally, the strategy used here could be extended to immobilize different enzymes in one microreactor for proteomic analysis as well as fabricating dual-enzymatic systems used as a platform to discover multitargeted enzyme-inhibitor drug lead compounds.

## Conflicts of interest

There are no conflicts of interest to declare.

## Acknowledgements

The authors are thankful for financial support from the Postgraduate Research & Practice Innovation Program of Jiangsu Province (KYCX17_0707).

## References

1 Q. Fu, K. Zhang, D. Gao, L. Wang, F. Yang, Y. Liu and Z. Xia, *Anal. Chim. Acta*, 2017, **969**, 63–71.
2 J. Zhou, B. Yang, J. Tang and W. Tang, *New J. Chem.*, 2018, **42**, 3526–3533.
3 E. J. Carrasco-Correa, E. F. Simo-Alfonso, G. Ramis-Ramos and J. M. Herero-Martinez, *Curr. Med. Chem.*, 2017, **24**, 781–795.
4 Z. Chen, T. Nishiyama, K. Uchiyama and T. Hobo, *Anal. Chim. Acta*, 2004, **501**, 17–23.
5 M. Lämmerhofer, F. Svec and J. M. J. Fréchet, *Anal. Chem.*, 2000, **72**, 4623–4628.
6 M. Guerrouache, M. C. Millot and B. Carbonnier, *Macromol. Rapid Commun.*, 2009, **30**, 109–113.
7 R. Noel Echevarria, E. J. Carrasco-Correa, S. Keunchkarian, M. Reta and J. M. Herrero-Martinez, *J. Sep. Sci.*, 2018, **41**, 1424–1432.
8 S. Dixit, I. S. Lee and J. H. Park, *J. Chromatogr. A*, 2017, **1507**, 132–140.
9 T. Koide and K. Ueno, *J. Chromatogr. A*, 2001, **909**, 305–315.
10 Y. Zheng, X. Wang and Y. Ji, *Talanta*, 2012, **91**, 7–17.
11 M. Kato, N. Matsumoto, K. Sakai-Kato and T. Toyo'oka, *J. Pharm. Biomed. Anal.*, 2003, **30**, 1845–1850.
12 M. Kato, H. Saruwatari, K. Sakai-Kato and T. Toyo'oka, *J. Chromatogr. A*, 2004, **1044**, 267–270.
13 J. Lu, F. Ye, A. Zhang, Z. Wei, Y. Peng and S. Zhao, *J. Sep. Sci.*, 2011, **34**, 2329–2336.
14 T. Hong, Y. Zheng, W. Hu and Y. Ji, *Anal. Biochem.*, 2014, **464**, 43–50.
15 R. Mallik, T. Jiang and D. S. Hage, *Anal. Chem.*, 2004, **76**, 7013–7022.
16 C. Yao, L. Qi, J. Qiao, H. Zhang, F. Wang, Y. Chen and G. Yang, *Talanta*, 2010, **82**, 1332–1337.
17 E. L. Pfaunmiller, M. Hartmann, C. M. Dupper, S. Soman and D. S. Hage, *J. Chromatogr. A*, 2012, **1269**, 198–207.
18 T. Hong, X. Chen, Y. Xu, X. Cui, R. Bai, C. Jin, R. Li and Y. Ji, *J. Chromatogr. A*, 2016, **1456**, 249–256.
19 E. Calleri, G. Massolini, D. Lubda, C. Temporini, F. Loiodice and G. Caccialanza, *J. Chromatogr. A*, 2004, **1031**, 93–100.
20 C. Temporini, E. Calleri, G. Fracchiolla, G. Carbonara, F. Loiodice, A. Lavecchia, P. Tortorella, G. Brusotti and G. Massolini, *J. Pharm. Biomed. Anal.*, 2007, **45**, 211–218.
21 R. Mallik, H. Xuan and D. S. Hage, *J. Chromatogr. A*, 2007, **1149**, 294–304.
22 L. Zhao, L. Yang and Q. Wang, *J. Chromatogr. A*, 2016, **1446**, 125–133.
23 T. Hong, C. Chi and Y. Ji, *J. Sep. Sci.*, 2014, **37**, 3377–3383.
24 S. Xu, R. Mo, C. Jin, X. Cui, R. Bai and Y. Ji, *J. Pharm. Biomed. Anal.*, 2017, **140**, 190–198.

 

25 C. Miao, R. Bai, S. Xu, T. Hong and Y. Ji, *J. Chromatogr. A*, 2017, **1487**, 227–234.
26 M. Ahmed and A. Ghanem, *Chirality*, 2014, **26**, 754–763.
27 Z. Liu, K. Otsuka, S. Terabe, M. Motokawa and N. Tanaka, *Electrophoresis*, 2002, **23**, 2973–2981.
28 C. Bi, X. Zheng, S. Azaria, S. Beeram, Z. Li and D. S. Hage, *Separations*, 2016, **3**, 27.
29 C. Bertucci and D. Tedesco, *Curr. Med. Chem.*, 2017, **24**, 743–757.
30 R. Mallik and D. S. Hage, *J. Pharm. Biomed. Anal.*, 2008, **46**, 820–830.
31 R. Isaksson, C. Pettersson, G. Pettersson, J. Ståhlberg, J. Hermansson and I. Marle, *Trends Anal. Chem.*, 1994, **13**, 431–439.
32 T. B. Vinzant, W. S. Adney, S. R. Decker, J. O. Baker, M. T. Kinter, N. E. Sherman, J. W. Fox and M. E. Himmel, *Appl. Biochem. Biotechnol.*, 2001, **91–93**, 99–107.
33 Y.-H. P. Zhang and L. R. Lynd, *Biotechnol. Bioeng.*, 2004, **88**, 797–824.
34 H. Matsunaga and J. Haginaka, *J. Chromatogr. A*, 2016, **1467**, 155–162.
35 Z. A. Alothman, A. Aqel, H. A. Al Abdelmoneim, A. Yacine Badjah-Hadj-Ahmed and A. A. Al-Warthan, *Chromatographia*, 2011, **74**, 1–8.
36 I. Gusev, X. Huang and C. Horvath, *J. Chromatogr. A*, 1999, **855**, 273–290.
37 E. Grushka, R. M. McCormick and J. J. Kirkland, *Anal. Chem.*, 1989, **81**, 241–246.
38 C. Pan, W. Lv, G. Wang, X. Niu, H. Guo and X. Chen, *J. Chromatogr. A*, 2017, **1484**, 98–106.
39 Y. Tian, C. Zhong, E. Fu and Z. Zeng, *J. Chromatogr. A*, 2009, **1216**, 1000–1007.
40 M. Kato, K. Sakai-Kato, N. Matsumoto and T. Toyo'oka, *Anal. Chem.*, 2002, **74**, 1915–1921.
41 D. Wang, X. Song, Y. Duan, L. Xu, J. Zhou and H. Duan, *Electrophoresis*, 2013, **34**, 1339–1342.
42 H. F. Li, H. Zeng, Z. Chen and J. M. Lin, *Electrophoresis*, 2009, **30**, 1022–1029.